Title

Reliable determination of site-specific in vivo protein N-glycosylation based on collision-induced MS/MS and chromatographic retention time.

Journal

Journal of the American Society for Mass Spectrometry, 25(5)

Authors

Wang, Benlian
Tsybovsky, Yaroslav
Palczewski, Krzysztof
et al.

Publication Date

2014-05-01

DOI

10.1007/s13361-013-0823-6

Peer reviewed

Published in final edited form as:
J Am Soc Mass Spectrom. 2014 May ; 25(5): 729–741. doi:10.1007/s13361-013-0823-6.

Reliable Determination of Site-specific *in vivo* Protein *N*-Glycosylation based on Collision-Induced MS/MS and Chromatographic Retention Time

Benlian Wang[1], **Yaroslav Tsybovsky**[2], **Krzysztof Palczewski**[1,2], and **Mark R. Chance**[1,*]

[1]Center for Proteomics and Bioinformatics, School of Medicine, Case Western Reserve University, Cleveland, Ohio 44106, United States

[2]Department of Pharmacology, School of Medicine, Case Western Reserve University, Cleveland, Ohio 44106, United States

Abstract

Site-specific glycopeptide mapping for simultaneous glycan and peptide characterization by MS is difficult because of the heterogeneity and diversity of glycosylation in proteins and the lack of complete fragmentation information for either peptides or glycans with current fragmentation technologies. Indeed, multiple peptide and glycan combinations can readily match the same mass of glycopeptides even with mass errors less than 5 ppm providing considerably ambiguity and analysis of complex mixtures of glycopeptides becomes quite challenging in the case of large proteins. Here we report a novel strategy to reliably determine site-specific *N*-glycosylation mapping by combining collision-induced dissociation (CID)-only fragmentation with chromatographic retention times of glycopeptides. This approach leverages an experimental pipeline with parallel analysis of glyco- and deglycopeptides. As the test case we chose ABCA4, a large integral membrane protein with 16 predicted sites for *N*-glycosylation. Taking advantage of CID features such as high scan speed and high intensity of fragment ions together combined with the retention times of glycopeptides to conclusively identify the non glycolytic peptide from which the glycopeptide was derived, we obtained virtually complete information about glycan compositions and peptide sequences, as well as the *N*-glycosylation site occupancy and relative abundances of each glycoform at specific sites for ABCA4. The challenges provided by this example provide guidance in analyzing complex relatively pure glycoproteins and potentially even more complex glycoprotein mixtures.

Introduction

Protein glycosylation, the covalent attachment of glycans to a protein, is one of the most common forms of post-translational modification and is implicated in various cellular processes including protein folding and trafficking, cellular signaling, recognition and adhesion [1]. Glycoproteins with glycans attached to Asn (*N*-glycosylation), and Ser or Thr

*To whom correspondence may be addressed: Mark R. Chance, Case Center for Proteomics and Bioinformatics, School of Medicine, Case Western Reserve University, 10900 Euclid Ave, Cleveland, OH 44106-4965. Tel.: 216-368-4406; Fax: 216-368-3812; mark.chance@case.edu.

residues (*O*-glycosylation) comprise over 50% of human proteins. Aberrant glycosylation has been reported to associate with various inherited and acquired diseases [2]. Mass spectrometry (MS) coupled with advanced separation methodology has emerged as the most powerful technology for glycosylation analyses [3–5]. The existing analytic pipelines focus on identifying glycans released from proteins by deglycosylation and/or glycopeptides obtained by protein digestion with proteases [6–7]. Unlike the direct glycan analysis, glycopeptide analyses can provide information about glycan composition at specific sites, which is crucial for detailed structural and functional information.

A number of studies have dealt with site-specific *N*-glycosylation mapping for simultaneous glycan and peptide characterization using MS [8–10]. Many analytical advances have been made in various steps including enzymatic proteolysis [11], glycopeptide enrichment [12–14], chromatographic fractionation and tandem MS/MS fragmentation [15–17]. In brief, high-resolution MS is essential for accurate glycopeptide mass assignments, and tandem MS is required to verify glycan composition or glycopeptide sequences through different fragmentation methods such as collision induced dissociation (CID), electron capture or transfer dissociation (ECD or ETD), higher energy collisional C-trap dissociation (HCD) and infrared multi-photon dissociation (IRMPD). A parallel analysis of deglycopeptides from PNGase F treatment in normal or O^{18} water can aid in the identification of *N*-glycosylation sites [13–14] and determination of site occupancy [18–19].

Basically, there are two critical unknowns for site-specific glycopeptide analysis that can be revealed by MS: the peptide mass and the glycan mass. ECD and ETD lead to fragmentation of the peptide backbone, but leave the sugar moieties intact, whereas CID mainly results in fragmentation of the sugar moieties but not the peptide. HCD allows detection of diagnostic oxonium ions and some product ions corresponding to the peptide backbone, which helps in glycosylation site identification but is less effective for determination of glycan structure [20–21]. None of these methods alone can achieve complete fragmentation and coverage for both peptides and glycans. Multiple peptide and glycan combinations are very likely to match the same glycopeptide mass, especially with complex mixtures of glycopeptides because of the heterogeneous nature of glycosylation and missing fragment ion information for either peptides or glycans. Correct assignment of glycopeptide composition and structure is still a key challenge for site-specific glycopeptide analysis by MS.

Recently, attempts have been made to employ the combination of CID and ETD to achieve in-depth characterization of glycopeptides by utilizing the advantages of these fragmentation techniques simultaneously, with CID employed for analyzing the glycans and ETD for sequencing the glycopeptide [22–23]. The key limitation of ETD is that this fragmentation method selectively favors higher-charge state precursor ions (plus three and above). This requirement is particularly problematic if the glycopeptides contain complex glycans with negatively charged NeuAc (sialic acid) or phosphorylated residues driving charge-state neutralization. In addition, long glycopeptides with high-charge-states needed for successful ETD fragmentation can host more than one glycosylation site, which will interfere with unambiguous site identification. More recently, a CID-HCD combined fragmentation approach has been applied to glycopeptide mapping [24]. Similarly, CID serves to analyze glycan composition and branching, whereas HCD primarily contributes to the identification

of glycosylation sites. In fact, HCD implemented in the Orbitrap generates fewer glycopeptide product ions for peptide sequencing. In a recent case confident assignment of glycosylation sites was achieved by MS3 analysis of the peptide-HexNAc ion (Y1) following MS2 by HCD [21,25]. Thus, in combined applications of either CID-ETD or CID-HCD, the ETD or HCD steps nicely complement CID.

In this study, we report a novel alternative strategy to reliably determine site-specific glycosylation based on the combination of CID-only fragmentation and known glycopeptide retention times. As a test case for the method, we chose the ATP-binding cassette transporter 4 from subfamily A of mammalian ABC transporters (ABCA4), an endogenous membrane protein from bovine retina with the molecular mass over 250 kDa (2281 amino acids) and sixteen theoretical *N*-linked glycosylation sites (N-X-S/T motif, where X can be any amino acid except proline). Previously, we reported the first systematic study of posttranslational modifications including phosphorylation and *N*-glycosylation in native ABCA4 [26]. Here, we focus on a strategy developed to achieve the correct and reliable assignments *N*-glycopeptide mapping of the protein based on collision-induced tandem MS in combination with chromatographic retention time. The results provide guidance for determining virtually complete information about glycan compositions and peptide sequences, as well as the *N*-glycosylation site occupancy and relative abundances of each glycoform at specific sites for a complex glycoprotein and possibly for moderately complex glycoprotein mixtures.

Experimental

Materials and Reagents

Dithiothreitol (DTT), iodoacetamide and PNGase F were purchased from Sigma-Aldrich. Sequencing grade modified trypsin and chymotrypsin were from Promega and Roche, respectively. All others chemicals and biochemical are from Sigma-Aldrich.

Preparation of ABCA4 samples from bovine rod outer segments

ABCA4 was prepared as described earlier [26]. Briefly, bovine rod outer segments (ROS) from frozen retinas were isolated under dim red light and homogenized in the hypotonic buffer (5 mM Bis-trispropane (BTP), pH 7.5, 1 mM DTT). ROS membranes were separated by centrifugation at 20,000 g for 30 min and solubilized with buffer composed of 20 mM BTP, pH 7.5, 10% glycerol, 30 mM NaCl, 1 mM DTT and 20 mM n-dodecyl- β-D-maltopyranoside (DDM).

Solubilized membranes were applied to a DE52 ion exchange column and washed with buffer containing 20 mM BTP, pH 7.5, 10% glycerol, 30 mM NaCl, 1 mM DTT and 1 mM DDM. The protein fraction containing ABCA4 was eluted with 150 mM NaCl in the same buffer and subjected to SDS-PAGE.

In-gel Digestions and Mass Spectrometry

Bovine ABCA4 was deglycosylated with commercially obtained PNGase F from *Elizabethkingia Meningoseptica* under denaturing conditions according to the manufacturer protocol. Cleavage of oligosaccharides was confirmed by a slight increase in ABCA4

mobility in SDS-PAGE gels (data not shown). Coomassie-stained SDS-PAGE gel pieces containing intact or PNGase F-treated ABCA4 were destained with 50% acetonitrile in 100 mM ammonium bicarbonate followed by 100% acetonitrile. Next, cysteine residues were reduced by incubating the sample with 20 mM DTT at room temperature for 60 min, followed by alkylation with 50 mM iodoacetamide for 30 min in the dark. The solution was removed and the gel pieces were washed with 100 mM ammonium bicarbonate and dehydrated in acetonitrile. Gel pieces were then dried in a SpeedVac centrifuge, rehydrated in 50 mM ammonium bicarbonate containing sequencing grade modified trypsin or chymotrypsin and left for overnight digestion at 37 °C. Proteolytic peptides were extracted from the gel with 50% acetonitrile in 5% formic acid, dried and reconstituted in 0.1% formic acid for MS analysis.

Liquid chromatography-tandem mass spectrometry analyses of the resulting peptides were performed with an LTQ Orbitrap XL linear ion trap mass spectrometer (Thermo Fisher Scientific, Waltham, MA) coupled to an Ultimate 3000 HPLC system (Dionex, Sunnyvale, CA). The digests were first trapped onto a C18 pre-column (PepMap100, 0.3 mm × 5 mm, 5 μm particle size, Dionex) and then equilibrated and desalted with 0.1 % formic acid for 4 min. The peptides were eluted on C18 Acclaim PepMap 100 column (0.075 mm × 150 mm; Dionex) with a linear gradient of acetonitrile from 2% to 60 % in60 min-long run at a flow rate of 0.3 μL/min. Spectra were acquired in the positive ionization mode by data-dependent methods consisting of a full MS scan in the high mass accuracy FT-MS mode (resolution: 100,000) and MS/MS scans of the five most abundant precursor ions in the CID mode at the normalized collision energy of 30%. The spray voltage was set at 2.4 kV. A dynamic exclusion function was applied with a repeat count of 2, repeat duration of 45 s, exclusion duration of 15 s, and exclusion size list of 350. The obtained data were submitted for a database search against the ABCA4 amino acid sequence using Mascot Daemon (Matrix Science, Boston, MA). Carbamidomethylation of Cys was set as a fixed modification, whereas oxidation of Met and conversion of Asn to Asp were selected as variable modifications. The mass tolerance was set as 10 ppm for precursor ions and 0.8 Da for product ions. Candidate *N*-linked-glycosylation sites were initially identified in deglycosylated peptides based on conversion of Asn residues to Asp by PNGase F. The corresponding glycosylated peptides were then identified by CID tandem MS. Sugar compositions of glycopeptides initially determined with GlycoMod software were further verified by manual interpretation of their MS/MS spectra.

Results

CID tandem mass spectra reveal the complete composition and some sequence information about the glycans in native N-glycopeptides

A typical CID tandem mass spectrum of an ABCA4 glycopeptide with the initial m/z of 1353.2650(3+) illustrating sequential loss of sugar moieties is shown in Supplemental Figure 1. In Supplemental Figure 1b, the fragment ions with m/z 1299.3 and 1867.7 can be easily recognized as triply and doubly charged parent glycopeptides with loss of one and two hexoses, respectively. The subsequent losses of hexoses followed by the dissociation of one HexNAc can be easily traced based on the fragment ions of either the triply charged

form (1299.3 → 1245.4 → 1191.3 →1137.6 → 1083.5 → 1029.6 → 975.5 → 921.3 → 867.3 → 799.7) or the doubly charged form (1867.7 → 1786.6 → 1706.0 → 1624.5 → 1543.9 → 1463.0 → 1381.5 → 1300.8 → 1198.9). Ions with m/z 799.7 and 1198.9 correspond to the triply and doubly charged (peptide + HexNAc) ions, respectively. The complete glycan composition $(Hex)_9(HexNAc)_2$ thus could be resolved and confirmed from both triply and doubly charged series of ions. On the other hand, high resolution of the full mass allows accurate determination of the charge state and monoisotopic mass of the parent ion, and therefore the mass of the glycopeptide, i.e. the sum of the masses of the peptide and glycan. The mass value of 2193.145 for the peptide itself derived from the calculated glycan mass subtracted from the measured mass of the glycopeptide matches ABCA4 peptide STEILQDLTDR^{1527}**N**VSDFLVK with a mass error of 1.511 ppm.

A hybrid type of *N*-glycopeptide was also examined and the CID tandem mass spectrum is shown in Figure1. The singly charged fragment ion m/z of 1885.9 was identified to result from losses of one NeuAc, one HexNAc and three Hex residues from the parent ion. The peptide ion carrying a single *N*-acetylglucosamine (m/z 1196.5), and also the most abundant fragment, was derived from the m/z 1885.9 fragment by losing three Hex and one HexNAc (m/z 1885.9 → 1723.8 → 1561.7 → 1399.6 → 1196.5). Similar to Supplemental Figure 1b, the glycan composition along with the conjugated peptide could be determined as $(NeuAc)(Hex)_6(HexNAc)_3$ + DIF^{504}**N**ITDR based on the fragment ions from CID tandem MS and the accurate full MS of the glycopeptide. Aside from these singly charged fragment ions, there was more rich information on doubly charged fragment ions. Among these, two major fragment ions (m/z 1352.6 and 1287.8) were derived directly from the doubly charged parent ion through the loss of Hex or NeuAc. Then following the loss of either NeuAc or Hex by separate pathways (m/z 1433.6 → 1352.6 → 1207.0 or m/z 1433.6 → 1287.8 → 1207.0), they reached the same fragment ion m/z of 1207.0. After one subsequent Hex loss from m/z 1207.0 to 1126.0, there was a further loss of Hex and HexNAc (m/z 1126.0 → 1045.0 → 943.4) to arrive at m/z 943.4 (m/z 1126.0 → 1024.3 → 943.4). This ion with m/z 934.4 corresponds to the peptide conjugated to three Hex and two HexNAc groups, a core structure for *N*-linked glycosylation. Thus, the entire sugar composition was verified by a series of doubly charged fragment ions. Alternatively, fragment ions with m/z 819.1 → 657.1 → 454.1 corresponding to NeuAc-Hex-HexNAc-Hex → NeuAc-Hex-HexNAc → NeuAc-Hex confirmed the presence of the NeuAc-Hex-HexNAc-Hex glycan, which appears associated with glycan sequence. However, caution is advisable because monosaccharide rearrangements may occur, and the situation will be more complex for large and highly branched glycans. In general, one should trust the glycan composition derived from the CID data, but not necessarily the structure assignment. Glycan structural determination requires the release of glycans prior to their LC/MS analysis.

Besides trypsin, we also performed glycoprotein digestion with chymotrypsin to increase sequence converge and obtain more information about each possible glycosylation site. Chymotrypsin mainly cuts at hydrophobic residues such as Trp, Tyr and Phe, and also slowly at Leu, and Met residues. Non-specific cleavage by chymotrypsin produces peptides with extensive sequence overlaps. As an example, the glycan moiety $(NeuAc)(Hex)_6(HexNAc)_3$ was observed conjugated to the same glycosylation site ^{504}Asn of

different peptides, in particular DIF^{504}**N**ITDR generated with trypsin digestion and NWRDIF^{504}**N**ITDRAL and NGPREGQADDVQNFNWRDIF^{504}**N**ITDRAL produced with chymotrypsin (Figures 1a–c). Mass errors for these assignments were 1.301, 1.463 and −1.168 ppm, respectively. Such protease digests by different or non-specific proteases that produce glycopeptides with varying lengths of the peptide portion but the same glycan portion, can serve as a secondary verification for site- specific glycosylation mapping [27].

CID tandem mass spectra help minimize the occurrence of false positives during assignment

There are sixteen potential *N*-glycosylation sites in ABCA4 with the consensus sequence Asn-X-Ser/Thr(X can be any amino acid except Pro) located at positions 14, 98, 415, 504, 950, 1455, 1527, 1586, 1660, 1732, 1803, 1817, 1931, 2005, 2050 and 2251. For complex digests of large proteins like ABCA4 carrying multiple NXS/T motifs, different combinations of glycans and peptides could match the same glycopeptide mass even when a high resolution mass spectrometer is employed. As an example, a glycopeptide with m/z 1213.2280(3+) has two possible assignments, both with a mass tolerance under 2 ppm (Figure 2a and Table 1). One is peptide STEILQDLTDR^{1527}**N**VSDFLVK + $(Hex)_3(Deoxyhexose)_1(HexNAc)_4$, and the other is peptide DKNPEEYGITVISQPL^{1660}**N**LTK + $(Hex)_6(HexNAc)_2$. However, the CID tandem mass spectrum of this glycopeptide shown in Figure 2b clearly shows six Hex losses from the parent ion (m/z 1213.2 → 1159.7 → 1105.5 → 1051.5 → 997.5 → 943.4 → 889.4) followed by another HexNAc residue loss leaving a (peptide + HexNAc) ion. Thus, only the latter assignment is supported by the MS/MS data. This result indicates that glycopeptide mapping cannot be solely based on a high resolution full MS; tandem MS is required to minimize false positive assignments [28].

It is generally accepted that characterization of glycoproteins by mass spectrometry is typically more difficult than the mass spectrometric analysis of proteins because of the extensive heterogeneity and lower ionization efficiency of glycoproteins [29]. Thus, glycopeptides are usually present in low abundance in MS data as compared to their corresponding non-glycosylated peptides. Many glycopeptide peaks are skipped in data-dependent LC-MS/MS runs. A challenging problem arises if the MS/MS spectrum of an individual glycopeptide lacks the quality to solve the complete glycan composition. To address this problem, LC-MS profiles of ABCA4 glyco- and de-glycopeptides were extracted as shown in Figure 3. A typical glycopeptide pattern appeared in the glycopeptide pool in which ions with m/z such as 1137.19(3+), 1191.21(3+), 1245.23(3+), 1299.25(3+) and 1353.27(3+) all differed by a mass of 162 Da, which corresponds to the mass of the Hex sugar residue. After PNGase F treatment, these glycopeptides disappeared and new peaks with m/z of 1097.57(2+) and 732.05(3+) (the latter is not shown in this m/z range) were formed corresponding to the same peptide with Asn converted to Asp by PNGase F. The deconvoluted tandem mass spectrum of ions with m/z 732.05(3+) or 1097.57(2+) confirmed the peptide sequence of STEILQDLTDR^{1527}**N/D**VSDFLVK (Supplemental Figure 2). That is, the glycopeptide ions listed above originated from the same peptide STEILQDLTDR^{1527}**N**VSDFLVK conjugated with different glycans. There was no free peptide observed in samples with or without PNGase F treatment, indicating 100%

occupancy of the ^{1527}Asn glycosylation site. The higher abundance fractions in the glycopeptide pool that allow determination of the entire glycan composition, such as 1353.27(3+) ion shown in Supplemental Figure 1, can help in interpreting and verifying other less abundant glycopeptides if their own MS/MS spectra cannot provide the entire glycan composition.

Reliable determination of site-specific in vivo N-glycosylation by CID tandem MS and HPLC retention time

As noted for all the glycopeptides we observed in ABCA4 and, previously, in the 5HT4R serotonin receptor, glycopeptides containing the same peptide but differing in their sugar chains almost always eluted as a single cluster during HPLC, with elution time differences spanning a couple of minutes [30]. Thus, we decided to determine site-specific *N*-glycosylation mapping by combining CID tandem MS with the HPLC retention times of glycopeptides. Table 2 displays another example of an ABCA4 glycopeptide with m/z of 1037.2098(4+) with multiple possible assignments. The extensive fragment ions observed in Figure 4 revealed the entire glycan composition of $(Hex)_9(HexNAc)_2$. For example, triply charged fragment ions with m/z from 1329.3 to 829.2 account for the sequential loss of nine Hex residues from the parent ion followed by a HexNAc residue loss (m/z 1329.3 with one Hex residue loss from the parent ion, then 1329.3 → 1274.9 → 1221.2 →1167.2 →1113.3 →1058.8 → 1005.3 → 951.2 → 896.7 → 829.2), which results in the peptide carrying a single *N*-acetylglucosamine (m/z 829.2). Assignment of the LLLWK^{14}**N**WTLRK + $(Hex)_{14}(HexNAc)_2$ glycopeptide could be easily excluded because of the incorrect glycan composition. Again, our results showed that CID MS/MS can be very helpful in minimizing the assignment of false positives.

In another case, two candidate glycopeptides had the same mass with an error less than 5 ppm and carried the same glycan moiety attached to different peptides, L^{950}**N**ITFYESQITAFLGHNGAGK or DKNPEEYGITVISQPL^{1660}**N**LTK. The only difference in the sugar portion was the presence of a sodium adduct (Figure 4). The fragment ion at m/z 509.3 in CID tandem MS corresponding to $Na(Hex)_3$ implied the existence of a sodium adduct, but the ion intensity was low, and no other sodium adducts were observed. Thus, it was very difficult to distinguish between these two possibilities based only on CID mass spectra. However, when we took the retention time into account (Figure 5), it was noted that the non-glycosylated L^{950}**N**ITFYESQITAFLGHNGAGK peptide with the m/z of 761.06 (3+) eluted at 43.82 min in the same LC-MS run, whereas the glycopeptide ion in question (m/z of 1037.2098(4+)) had a retention time around 36.11 min. Although the addition of a high mannose type sugar moiety and a Na adduct could result in a slight retention time change, a 7 min difference between the same peptide with and without such a polysaccharide in the same LC/MS run is far too great. On the other hand, a glycopeptide with the m/z of 1375.2804(3+) uniquely representing the DKNPEEYGITVISQPL^{1660}**N**LTK + $(Hex)_9(HexNAc)_2$ conjugate was observed with a retention time around 36.05 min, only 0.06 min different from that of the 1037.2098(4+) ion. Furthermore, the corresponding DKNPEEYGITVISQPL^{1660}**N/D**LTK peptide deglycosylated with PNGase F eluted at 38.84 min, only 2.79 min apart from its glycopeptide in a separate LC/MS run. This small difference could be attributed to the

conversion of Asn to Asp [31]. The peptide sequence and the N/D conversion were confirmed by the tandem MS shown in Supplemental Figure 3. Hence, by combining the information from CID tandem MS with retention times of glycopeptides, we were able to confidently assign 1037.2098(4+) ion to the DKNPEEYGITVISQPL^{1660}**N**LTK + Na $(Hex)_9(HexNAc)_2$ glycopeptide.

Another important result provided in Figure 3 is that the deglycosylated peptide with the Asn converted to an Asp by PNGase F actually appears at the same retention time range of 38–41 min with its clustered glycopeptides even in a separate LC-MS run. Deconvolution of the CID tandem mass spectrum of this deglycosylated peptide, which is usually easier to obtain compared to its glycoforms, can clearly reveal the peptide sequence. Moreover, if a glycosylation site is only partially occupied as we previously observed in the 5HT4R serotonin receptor [30], the same peptide with and without attached saccharides can be identified in a single LC-MS run. In such a case, determination of the un-glycosylated peptide is simple because the retention time of the root peptide is close to that of its glycoform without the delay introduced by the Asn to Asp conversion [30]. Identification of the glycosylation site and glycopeptide can then be confirmed based on the retention times of un- or de-glycosylated root peptide. Thus, the addition of HPLC retention time data could provide a solution to the problem of CID tandem MS of lacking sufficient peptide information for accurate glycopeptide mapping.

Discussion

Among the now-used fragmentation modes, only CID can provide complete glycan composition, whereas alternative fragmentation modes like HCD, ETD and ECD function primarily to identify glycopeptide or glycosylation sites. Moreover, CID is the most routinely used method with the most rapid acquisition speed and the highest intensity of product ions. This mode can provide an average scan speed over 2 times faster than HCD [32] and a signal intensity 10 times higher than ETD spectra for the same peptide fragmentation [33]. Thus, the CID-retention time approach can be beneficial for characterization of low-abundance glycopeptides. In addition, LC-MS analysis of corresponding deglycosylated peptides from PNGase F treatment in normal or O^{18}water is already included in the standard experimental pipeline for site-specific glycosylation mapping to screen *N*-glycosylation sites and calculate their occupancies. No additional experimental steps are required to determine the retention times of deglycosylated peptides.

Factors influencing the retention time of glycopeptides

Obviously, the HPLC retention time of a glycopeptide depends on the properties of its components, the glycan and the peptide. However, these components differentially affect the retention time. As shown in Figure 6, addition of hexose and HexNAc sugar residues causes a glycopeptide to elute earlier, a phenomenon attributable to the hydrophilic character of the sugar moieties. In contrast, the presence of NeuAc or a phospho- group on the glycan chain results in an increase in retention time, as the negatively-charged NeuAc and phospho groups counteract the positive charge of the glycopeptide proton, resulting in a tighter binding to the reversed phase HPLC matrix. For example, addition of one NeuAc or

phospho group shifts the retention time of glycopeptide DIF^{504}**N**ITDR from 32.02 min to 36.86 or 37.68 min, respectively. The larger the glycan moiety, the greater the effect it has on the retention time of a glycopeptide. However, this generality does not seem to apply to Hex and HexNAc saccharides. For instance, the retention time of glycopeptide STEILQDLTDR^{1527}**N**VSDFLVK changes from 39.36 only slightly to 39.09 min due to an increase in Hex residues from five to nine. The peptide component also has a major influence on the retention time of a glycopeptide. Examples of a strong peptide effect on the retention time are shown in Figure 6 and Table 3. Retention times of 25.41, 36.27, 39.30 and 50.91 min correspond to the same glycan $(Hex)_6(HexNAc)_2$ conjugated to peptides NA^{415}**N**STFEELER, DKNPEEYGITVISQPL^{1527}**N**LTK, STEILQDLTDR^{1527}**N**VSDFLVK, and LPAPPFTGEALVGFLSDLGQLM^{1586}**N**VSGGPMTR, respectively. The retention time of a glycopeptide strongly depends on its size and composition, as well as the physical and chemical properties of its amino acids. Thus, it is the peptide component rather than the attached glycans (with an exception for those altering the charge, such as NeuAc and phosphor- groups) that primarily contributes to the retention time of the corresponding glycopeptide. This fact enables glycopeptide identification based on comparison with retention time of the corresponding un- or de-glycosylated peptide.

Retention time-based prediction of peptides has been applied in proteomics to improving confidence in peptide identification in shotgun experiments [34–35]. Attempts also have been made to use retention time predictions for peptides with some post-translational modifications such as acetylation, methylation, oxidation and phosphorylation [36–39]. Of course, the more hydrophobic the peptide, the more organic solvent is required to elute it from a reversed-phase column. A linear dependence of peptide retention times on peptide mass is often observed when linear gradients are used in reversed-phase chromatography [40]. For post-translational modifications that do not alter charge, it is reasonable to expect modest changes in retention time [41], with the exception of Met oxidation [42]. This is in agreement with our observation of retention time changes for glycopeptides.

In addition to its retention time, the apparent relative abundance of each glycoform at a specific site can also be calculated from the area under the corresponding HPLC peak (with an assumption of modest variation in ionization efficiencies), which is essential to understanding the structure and function of glycoproteins. Since no glycopeptide enrichment was performed in our study, there were no associated shifts in the glycopeptide yields. The resulting site-specific glycopeptide mapping of ABCA4 includes identification of *N*-glycosylation sites, glycan compositions, apparent *N*-glycosylation site occupancies and apparent relative abundances of each polysaccharide detected for a single site (Table 3). The corresponding experimental pipeline is presented in Scheme 1. Here we focus especially on the strategy to achieve reliable *N*-glycosylation mapping, since the standard approaches to determine site-specific glycosylation have been well reviewed [43]. In our case, glycoproteins and their corresponding deglycosylated proteins were simply separated by SDS PAGE, the target protein band was ‘in-gel’ digested, and MS analysis based on CID-only fragmentation and chromatographic retention time was performed. First, a high-resolution full MS provides a highly accurate glycopeptide mass with an error within 5 ppm.

Then, a complete glycan fragmentation by CID tandem MS allows the correct assignment of glycan composition. Thus, the peptide mass is calculated by subtracting the entire glycan mass from the glycopeptide mass. Candidate glycosylated peptides then were initially proposed based on this peptide mass and the known protein sequence. Finally, identification of the peptide confirmed based on the retention time of either the un-glycosylated peptide in the same LC-MS/MS run in the case of partial occupancy of the corresponding site, or that of the deglycosylated peptide in a separate LC-MS/MS run if the site is fully glycosylated. Furthermore, in addition to proteolysis with a specific protease (usually trypsin), a non-specific protease such as chymotrypsin can be employed. Verification of the glycopeptide assignment then is accomplished by utilizing different proteases (which can have varying specificity), which generate peptides of varying lengths with extensive sequence overlaps. The use of different enzymes for digestion is necessary for our analytical strategy, not only to cover most of the potential glycosylation sites, but also to assist in assigning each glycosylation site to different glycopeptides.

Notably, these unequivocal assignments were made without the input of protein structure or topological model information, which can be very advantageous for studies of poorly characterized proteins. In the case of ABCA4, however, the known membrane topology [26]was used to validate our *N*-glycosylation mapping. Among sixteen potential N-glycosylated sites in ABCA4, seven are found *N*-glycosylated (with further glycan compositions solved for six of them) and eight are un-glycosylated. In complete agreement with this topological model, all the detected *N*-glycosylation sites were found situated in the exo-cytoplasmic protein regions, whereas none of the theoretical *N*-glycosylation sites in the cytoplasm were shown to be glycosylated. The only undetected site is Asn1732 located in a short loop that connects two transmembrane helices. Such a location makes it difficult to obtain the corresponding peptide by enzymatic digestion.

Since no glycopeptide enrichment was performed here, all un-glycosylated peptides were also available for analysis. Thus, protein identification should be easily achieved by a simple database search without the input of any glycosylation information. Thus, our CID-retention time approach works well for known and unknown proteins and is not limited to a single protein. It could face a greater challenge for glycoproteomic studies with large number of glycopeptides in the mixture. However, with the assistance of increasing structural data about investigated proteins available in the literature and the development of software for retention time predictions, coupled to continuing improvements in instrumentation, our approach is expected to provide valuable information for analysis of protein mixtures as well.

Conclusions

In summary, we present a comprehensive approach to site-specific *N*-glycopeptide mapping that allows simultaneous glycan and peptide characterization by combining CID tandem mass spectrometry with the HPLC retention times of glycopeptides. The former can provide the entire glycan composition, and the latter can assist in identifying the root peptide from which the glycopeptide is derived. Detailed information about *N*-glycosylation sites, glycan compositions and occupancies as well as relative abundances of each glycoform at a specific

site was obtained based on just two parallel analyses of glycosylated and deglycosylated peptides.

Supplementary Material

Refer to Web version on PubMed Central for supplementary material.

Acknowledgments

We are grateful to Dr. Leslie T. Webster, Jr., for critical comments.

This publication was made possible in part through support by the National Institute for Allergy and Infectious Diseases (Center for AIDS Research Proteomics Core, P30-AI-036219), the National Cancer Institute (Cancer Center Proteomics Core, P30-CA-043703) and the National Institute for Biomedical Imaging and Bioengineering (R01-EB-09866) (to M.R.C.) and the National Eye Institute of the National Institutes of Health under award numbers of R01EY009339 and P30EY11373 (to K.P.). K.P. is John H. Hord Professor of Pharmacology. M.R.C. is Charles W. and Iona A. Mathias Professor of Cancer Research.

References

1. Bielik AM, Zaia J. Historical overview of glycoanalysis. Methods Mol Biol. 2010; 600:9–30. [PubMed: 19882118]
2. Ohtsubo K, Marth JD. Glycosylation in cellular mechanisms of health and disease. Cell. 2006; 126(5):855–67. [PubMed: 16959566]
3. Leymarie N, Zaia J. Effective use of mass spectrometry for glycan and glycopeptide structural analysis. Anal Chem. 2012; 84(7):3040–8. [PubMed: 22360375]
4. Wuhrer M. Glycomics using mass spectrometry. Glycoconj J. 2013; 30(1):11–22. [PubMed: 22532006]
5. Pan S, Chen R, Aebersold R, Brentnall TA. Mass spectrometry based glycoproteomics--from a proteomics perspective. Mol Cell Proteomics. 2011; 10(1):R110 003251. [PubMed: 20736408]
6. Morelle W, Michalski JC. Analysis of protein glycosylation by mass spectrometry. Nat Protoc. 2007; 2(7):1585–602. [PubMed: 17585300]
7. Ruhaak LR, Huhn C, Koeleman CA, Deelder AM, Wuhrer M. Robust and high-throughput sample preparation for (semi-)quantitative analysis of N-glycosylation profiles from plasma samples. Methods Mol Biol. 2012; 893:371–85. [PubMed: 22665312]
8. Desaire H. Glycopeptide analysis, recent developments and applications. Mol Cell Proteomics. 2013; 12(4):893–901. [PubMed: 23389047]
9. Zhao J, Liu YH, Reichert P, Pflanz S, Pramanik B. Glycosylation analysis of interleukin-23 receptor: elucidation of glycosylation sites and characterization of attached glycan structures. J Mass Spectrom. 2010; 45(12):1416–25. [PubMed: 21053369]
10. Go EP, Chang Q, Liao HX, Sutherland LL, Alam SM, Haynes BF, Desaire H. Glycosylation site-specific analysis of clade C HIV-1 envelope proteins. J Proteome Res. 2009; 8(9):4231–42. [PubMed: 19610667]
11. Nwosu CC, Huang J, Aldredge DL, Strum JS, Hua S, Seipert RR, Lebrilla CB. In-gel Nonspecific Proteolysis for Elucidating Glycoproteins (INPEG) - A Method for Targeted Protein-Specific Glycosylation Analysis in Complex Protein Mixtures. Anal Chem. 2012
12. Zhang H, Li XJ, Martin DB, Aebersold R. Identification and quantification of N-linked glycoproteins using hydrazide chemistry, stable isotope labeling and mass spectrometry. Nat Biotechnol. 2003; 21(6):660–6. [PubMed: 12754519]
13. Kaji H, Saito H, Yamauchi Y, Shinkawa T, Taoka M, Hirabayashi J, Kasai K, Takahashi N, Isobe T. Lectin affinity capture, isotope-coded tagging and mass spectrometry to identify N-linked glycoproteins. Nat Biotechnol. 2003; 21(6):667–72. [PubMed: 12754521]

14. Zielinska DF, Gnad F, Wisniewski JR, Mann M. Precision mapping of an in vivo N-glycoproteome reveals rigid topological and sequence constraints. Cell. 2010; 141(5):897–907. [PubMed: 20510933]
15. Ding W, Nothaft H, Szymanski CM, Kelly J. Identification and quantification of glycoproteins using ion-pairing normal-phase liquid chromatography and mass spectrometry. Mol Cell Proteomics. 2009; 8(9):2170–85. [PubMed: 19525481]
16. Wada Y, Azadi P, Costello CE, Dell A, Dwek RA, Geyer H, Geyer R, Kakehi K, Karlsson NG, Kato K, Kawasaki N, Khoo KH, Kim S, Kondo A, Lattova E, Mechref Y, Miyoshi E, Nakamura K, Narimatsu H, Novotny MV, Packer NH, Perreault H, Peter-Katalinic J, Pohlentz G, Reinhold VN, Rudd PM, Suzuki A, Taniguchi N. Comparison of the methods for profiling glycoprotein glycans--HUPO Human Disease Glycomics/Proteome Initiative multi-institutional study. Glycobiology. 2007; 17(4):411–22. [PubMed: 17223647]
17. Leymarie N, Griffin PJ, Jonscher K, Kolarich D, Orlando R, McComb M, Zaia J, Aguilan J, Alley WR, Altmann F, Ball LE, Basumallick L, Bazemore-Walker CR, Behnken H, Blank MA, Brown KJ, Bunz SC, Cairo CW, Cipollo JF, Daneshfar R, Desaire H, Drake RR, Go EP, Goldman R, Gruber C, Halim A, Hathout Y, Hensbergen PJ, Horn DM, Hurum D, Jabs W, Larson G, Ly M, Mann BF, Marx K, Mechref Y, Meyer B, Moginger U, Neususs C, Nilsson J, Novotny MV, Nyalwidhe JO, Packer NH, Pompach P, Reiz B, Resemann A, Rohrer JS, Ruthenbeck A, Sanda M, Schulz JM, Schweiger-Hufnagel U, Sihlbom C, Song E, Staples GO, Suckau D, Tang H, Thaysen-Andersen M, Viner RI, An Y, Valmu L, Wada Y, Watson M, Windwarder M, Whittal R, Wuhrer M, Zhu Y, Zou C. Interlaboratory Study on Differential Analysis of Protein Glycosylation by Mass Spectrometry: the ABRF Glycoprotein Research Multi-Institutional Study 2012. Mol Cell Proteomics. 2013
18. Pan S, Tamura Y, Chen R, May D, McIntosh MW, Brentnall TA. Large-scale quantitative glycoproteomics analysis of site-specific glycosylation occupancy. Mol Biosyst. 2012; 8(11): 2850–6. [PubMed: 22892896]
19. Bailey UM, Jamaluddin MF, Schulz BL. Analysis of congenital disorder of glycosylation-Id in a yeast model system shows diverse site-specific under-glycosylation of glycoproteins. J Proteome Res. 2012; 11(11):5376–83. [PubMed: 23038983]
20. Hart-Smith G, Raftery MJ. Detection and characterization of low abundance glycopeptides via higher-energy C-trap dissociation and orbitrap mass analysis. J Am Soc Mass Spectrom. 2012; 23(1):124–40. [PubMed: 22083589]
21. Segu ZM, Mechref Y. Characterizing protein glycosylation sites through higher-energy C-trap dissociation. Rapid Commun Mass Spectrom. 2010; 24(9):1217–25. [PubMed: 20391591]
22. Mechref Y. Use of CID/ETD mass spectrometry to analyze glycopeptides. Curr Protoc Protein Sci. 2012; Chapter 12(Unit 12 11):1–11.
23. Hogan JM, Pitteri SJ, Chrisman PA, McLuckey SA. Complementary structural information from a tryptic N-linked glycopeptide via electron transfer ion/ion reactions and collision-induced dissociation. J Proteome Res. 2005; 4(2):628–32. [PubMed: 15822944]
24. Scott NE, Parker BL, Connolly AM, Paulech J, Edwards AV, Crossett B, Falconer L, Kolarich D, Djordjevic SP, Hojrup P, Packer NH, Larsen MR, Cordwell SJ. Simultaneous glycan-peptide characterization using hydrophilic interaction chromatography and parallel fragmentation by CID, higher energy collisional dissociation, and electron transfer dissociation MS applied to the N-linked glycoproteome of Campylobacter jejuni. Mol Cell Proteomics. 2011; 10(2):M000031–MCP201. [PubMed: 20360033]
25. Mayampurath AM, Wu Y, Segu ZM, Mechref Y, Tang H. Improving confidence in detection and characterization of protein N-glycosylation sites and microheterogeneity. Rapid Commun Mass Spectrom. 2011; 25(14):2007–19. [PubMed: 21698683]
26. Tsybovsky Y, Wang B, Quazi F, Molday RS, Palczewski K. Posttranslational modifications of the photoreceptor-specific ABC transporter ABCA4. Biochemistry. 2011; 50(32):6855–66. [PubMed: 21721517]
27. Nwosu CC, Seipert RR, Strum JS, Hua SS, An HJ, Zivkovic AM, German BJ, Lebrilla CB. Simultaneous and extensive site-specific N- and O-glycosylation analysis in protein mixtures. J Proteome Res. 2011; 10(5):2612–24. [PubMed: 21469647]

28. Desaire H, Hua D. When can glycopeptides be assigned based solely on high-resolution mass spectrometry data? International Journal of Mass Spectrometry. 2009; 287(1–3):21–26.
29. Morelle W, Michalski JC. Glycomics and mass spectrometry. Curr Pharm Des. 2005; 11(20): 2615–45. [PubMed: 16101462]
30. Salom D, Wang B, Dong Z, Sun W, Padayatti P, Jordan S, Salon JA, Palczewski K. Post-translational modifications of the serotonin type 4 receptor heterologously expressed in mouse rod cells. Biochemistry. 2012; 51(1):214–24. [PubMed: 22145929]
31. Dasari S, Wilmarth PA, Rustvold DL, Riviere MA, Nagalla SR, David LL. Reliable detection of deamidated peptides from lens crystallin proteins using changes in reversed-phase elution times and parent ion masses. J Proteome Res. 2007; 6(9):3819–26. [PubMed: 17696381]
32. Jedrychowski MP, Huttlin EL, Haas W, Sowa ME, Rad R, Gygi SP. Evaluation of HCD- and CID-type fragmentation within their respective detection platforms for murine phosphoproteomics. Mol Cell Proteomics. 2011; 10(12):M111 009910. [PubMed: 21917720]
33. Kim MS, Zhong J, Kandasamy K, Delanghe B, Pandey A. Systematic evaluation of alternating CID and ETD fragmentation for phosphorylated peptides. Proteomics. 2011; 11(12):2568–72. [PubMed: 21598390]
34. Palmblad M, Ramstrom M, Bailey CG, McCutchen-Maloney SL, Bergquist J, Zeller LC. Protein identification by liquid chromatography-mass spectrometry using retention time prediction. J Chromatogr B Analyt Technol Biomed Life Sci. 2004; 803(1):131–5.
35. Goloborodko AA, Mayerhofer C, Zubarev AR, Tarasova IA, Gorshkov AV, Zubarev RA, Gorshkov MV. Empirical approach to false discovery rate estimation in shotgun proteomics. Rapid Commun Mass Spectrom. 2010; 24(4):454–62. [PubMed: 20069687]
36. Moruz L, Staes A, Foster JM, Hatzou M, Timmerman E, Martens L, Kall L. Chromatographic retention time prediction for posttranslationally modified peptides. Proteomics. 2012; 12(8):1151–9. [PubMed: 22577017]
37. Lengqvist J, Eriksson H, Gry M, Uhlen K, Bjorklund C, Bjellqvist B, Jakobsson PJ, Lehtio J. Observed peptide pI and retention time shifts as a result of post-translational modifications in multidimensional separations using narrow-range IPG-IEF. Amino Acids. 2011; 40(2):697–711. [PubMed: 20725754]
38. Chen VC, Chou CC, Hsieh HY, Perreault H, Khoo KH. Targeted identification of phosphorylated peptides by off-line HPLC-MALDI-MS/MS using LC retention time prediction. J Mass Spectrom. 2008; 43(12):1649–58. [PubMed: 18613259]
39. Kiselar JG, Janmey PA, Almo SC, Chance MR. Structural analysis of gelsolin using synchrotron protein footprinting. Mol Cell Proteomics. 2003; 2(10):1120–32. [PubMed: 12966145]
40. Palmblad M. Retention time prediction and protein identification. Methods Mol Biol. 2007; 367:195–207. [PubMed: 17185777]
41. Yang L, Tu S, Ren C, Bulloch EM, Liao CL, Tsai MD, Freitas MA. Unambiguous determination of isobaric histone modifications by reversed-phase retention time and high-mass accuracy. Anal Biochem. 2010; 396(1):13–22. [PubMed: 19699711]
42. Xu G, Takamoto K, Chance MR. Radiolytic modification of basic amino acid residues in peptides: probes for examining protein-protein interactions. Anal Chem. 2003; 75(24):6995–7007. [PubMed: 14670063]
43. An HJ, Froehlich JW, Lebrilla CB. Determination of glycosylation sites and site-specific heterogeneity in glycoproteins. Curr Opin Chem Biol. 2009; 13(4):421–6. [PubMed: 19700364]

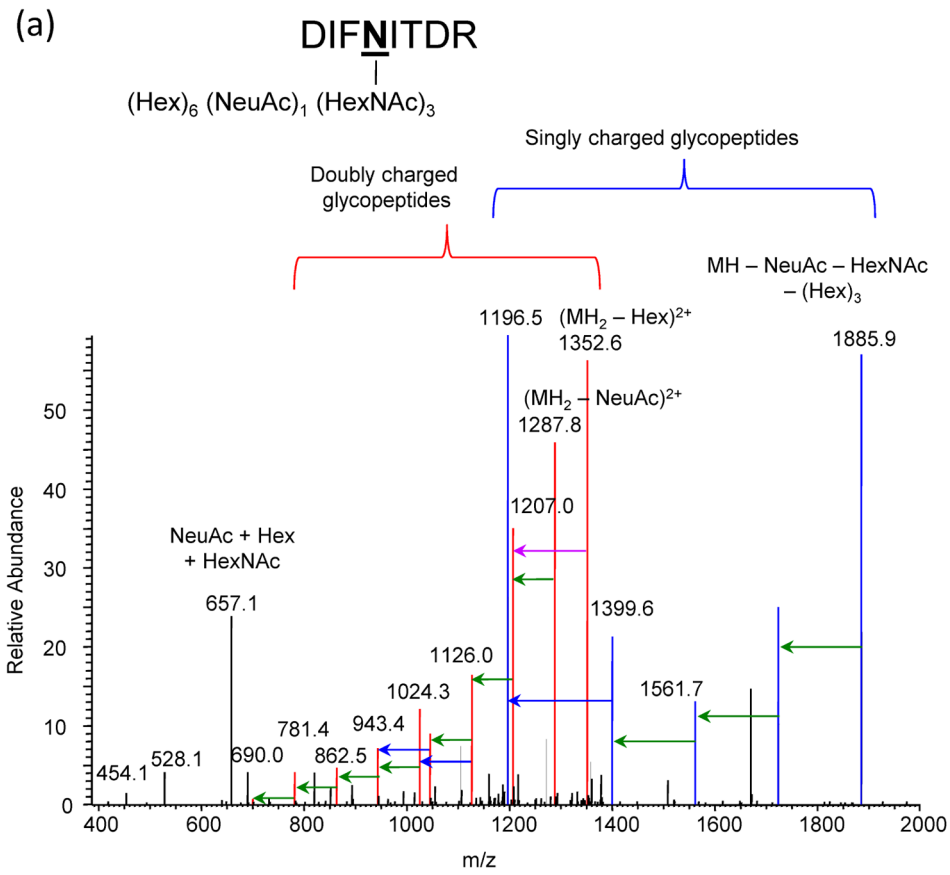

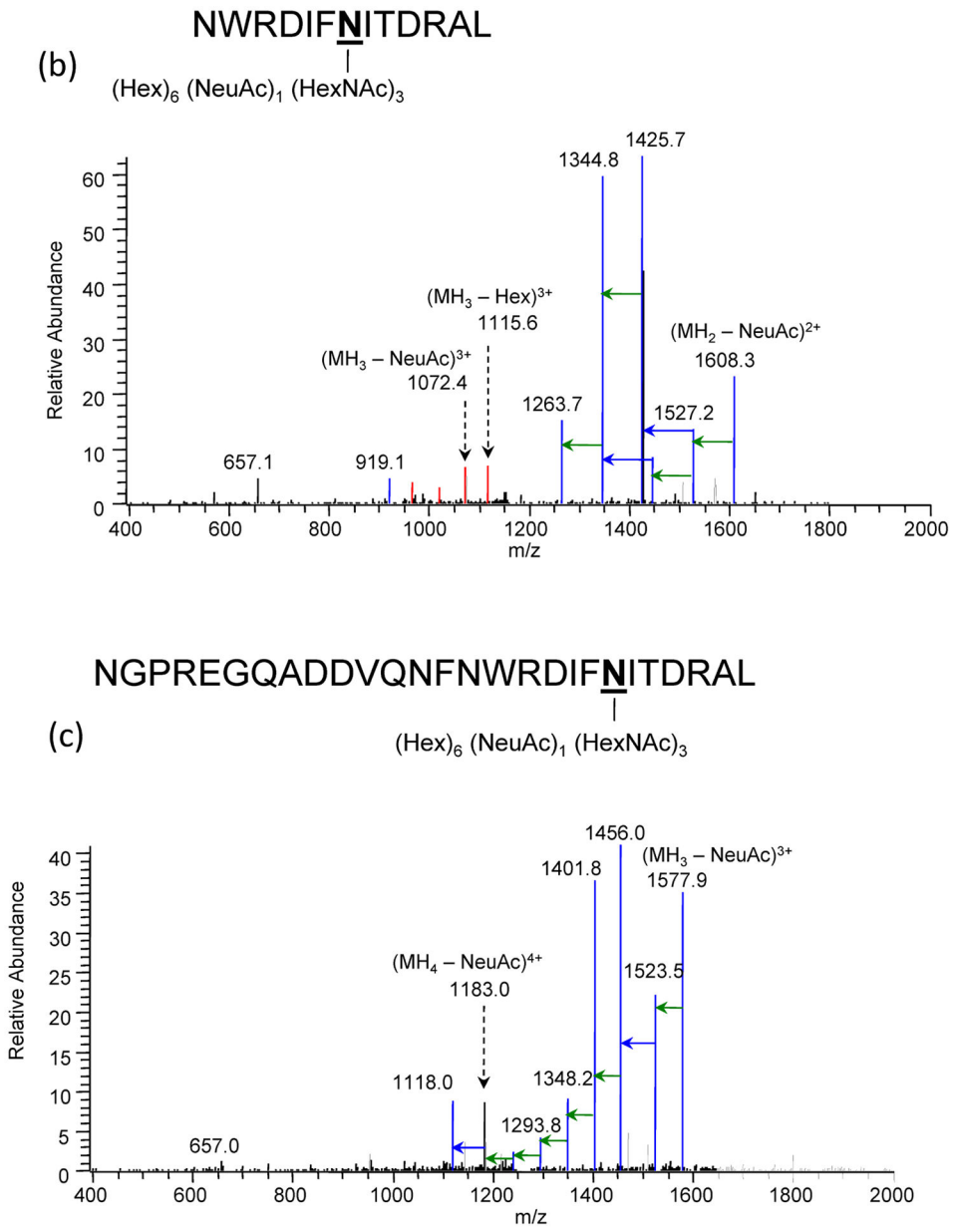

Figure 1.

Mass spectra of hybrid type glycans attached to different ABCA4 peptides at ^{504}Asn : (a) DIF^{504}**N**ITDR from trypsin digestion, (b) NWRDIF^{504}**N**ITDRAL and (c) NGPREGQADDVQNFNWRDIF^{504}**N**ITDRAL from chymotrypsin digestion. Green, blue and purple arrows represent the loss of Hex, HexNAc and NeuAc residues, respectively.

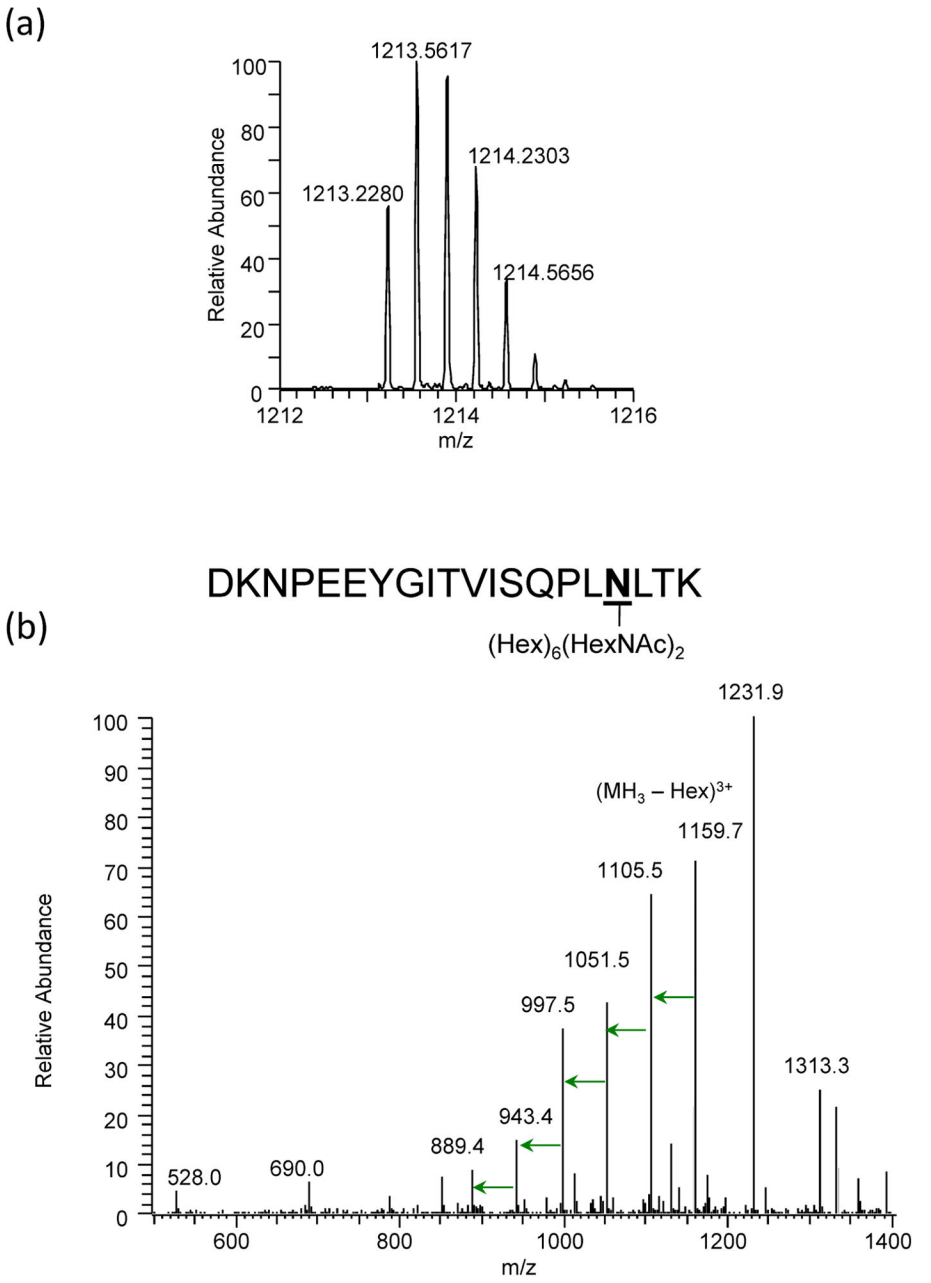

Figure 2.

Full MS (a) and CID MS/MS (b) mass spectra of an ABCA4 glycopeptide with the parent ion m/z of 1213.2280(3+).

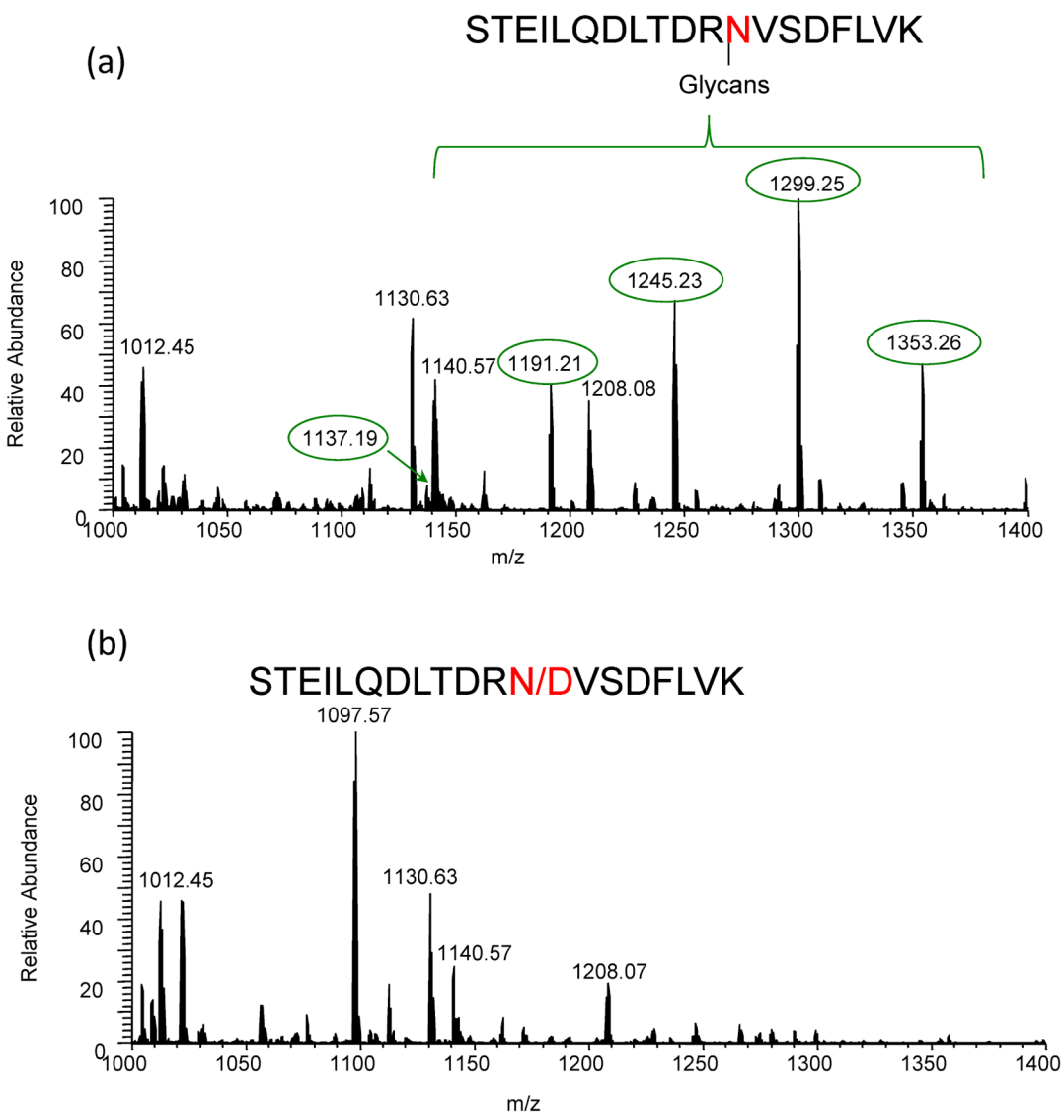

Figure 3.

Full MS of the glycosylated (a) and deglycosylated (b) ABCA4 peptide STEILQDLTDR[1527]**N**VSDFLVK eluting at 38–41 min. The peak at m/z 1097.57(2+) corresponds to the deglycosylated peptide with a mass shift of 0.980 Da because of the conversion of [1527]Asn to an Asp residue due to PNGase F treatment.

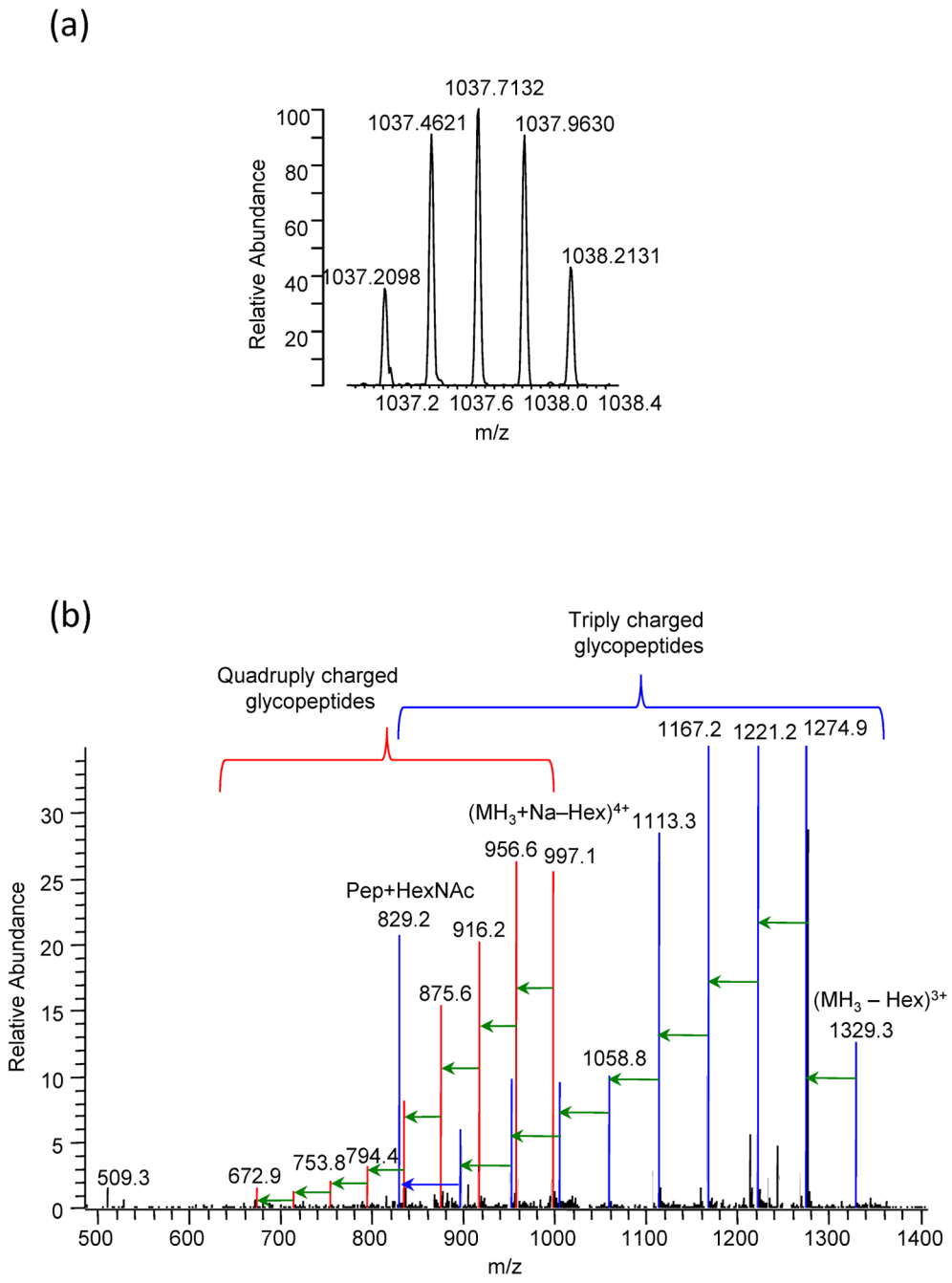

Figure 4.

Full MS (a) and CID MS/MS (B) spectra of an ABCA4 glycopeptide with parent ion m/z 1037.2098(4+).

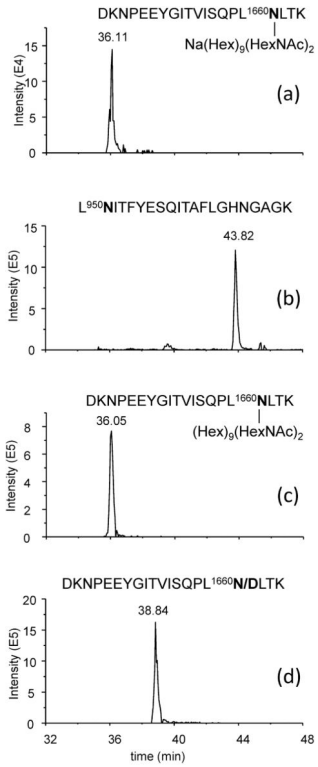

Figure 5.

Comparison of retention time of (a) the 1037.2098(4+) ion introduced in Figure 4; (b): peptide L^{950}**N**ITFYESQITAFLGHNGAGK; (c): Glycopeptide DKNPEEYGITVISQPL^{1660}**N**LTK+ $(Hex)_9(HexNAc)_2$; (d): peptide DKNPEEYGITVISQPL^{1660}**N/D**LTK from PNGase F treated sample in a separate LC/MS run.

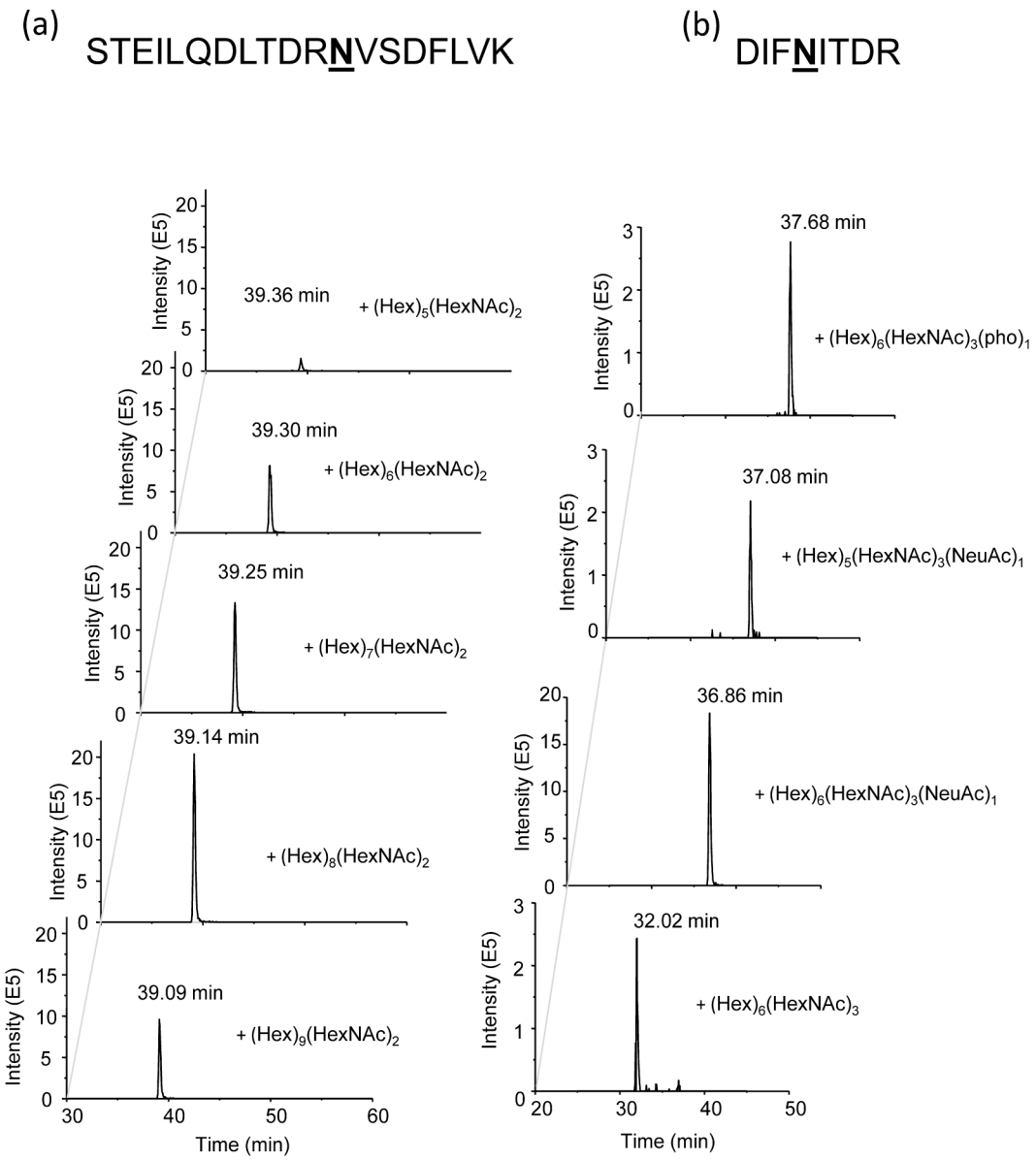

Figure 6.

Retention time of glycopeptides (a) STEILQDLTDR[1527]**N**VSDFLVK with high mannose type of glycosylation and DIF[504]**N**ITDR with hybrid type glycosylation (b).

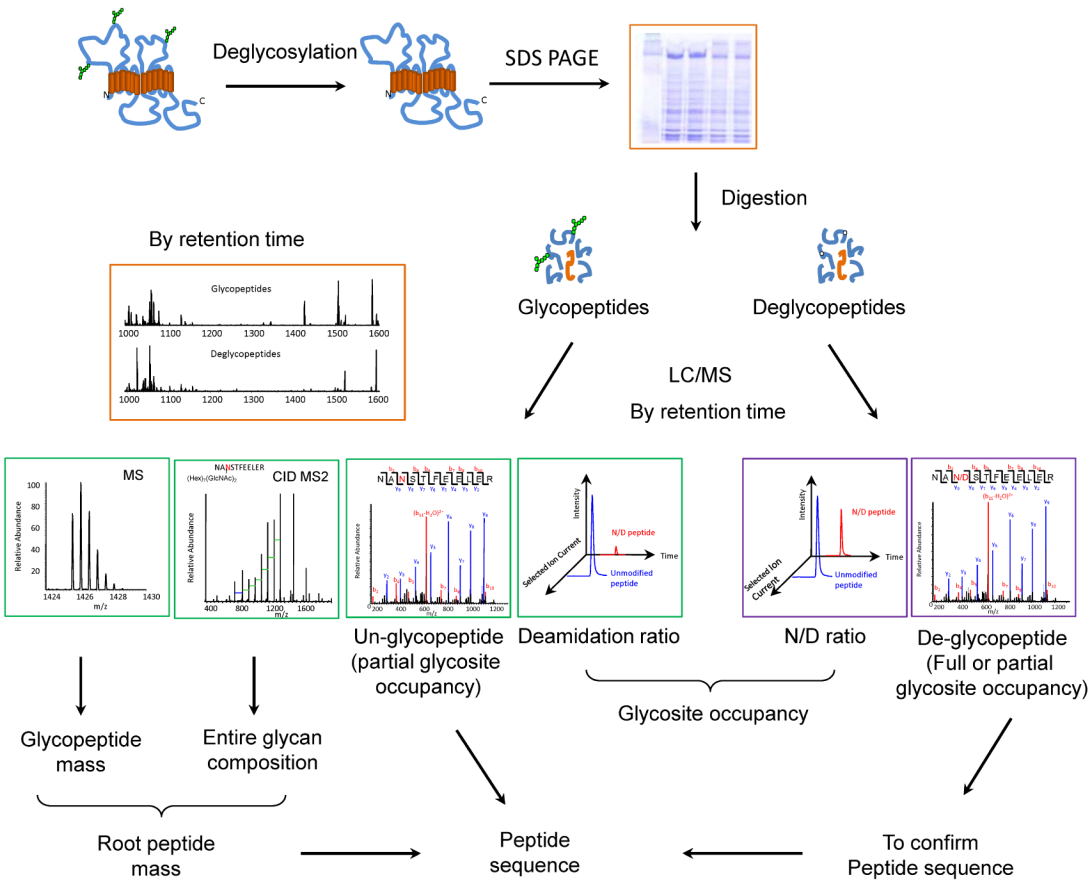

Scheme 1.

The experimental pipeline for site-specific *N*-glycopeptide mapping using CID-retention time approach. See main text for details.

Table 1

Two ABCA4 glycopeptides that can be assigned to the same parent ion with m/z of 1213.2280(3+), creating ambiguity in glycopeptide mapping. The mass error is under 2 ppm in both cases.

Observed GP mass	Peptide sequence	Glyco site	Glycan composition	Theoretical GP mass	Error (ppm)
3637.669	STEILQDLTDR**N**VSDFLVK	Asn 1527	$(Hex)_3(Deoxyhexose)_1(HexNAc)_4$	3637.673	−1.173
	DKNPEEYGITVISQPL**N**LTK	Asn 1660	$(Hex)_6(HexNAc)_2$	3637.663	1.746

Table 2

List of potential ABCA4 glycopeptides with the parent ion m/z of 1037.2098(4+) matching the same theoretical mass.

Observed GP mass	Peptide sequence	Glyco site	Glycan composition	Theoretical GP mass	Error (ppm)
4145.8158	LLLWKNWTLRK	Asn 14	$(Hex)_{14}(HexNAc)_2$	4145.792	5.676
	LNITFYESQITAFLGHNGAGK	Asn 950	$(Hex)_9(HexNAc)_2$	4145.795	4.952
	DKNPEEYGITVISQPLNLTK	Asn 1660	$Na(Hex)_9(HexNAc)_2$	4145.803	3.143

Table 3

Summary of N-glycosylation mapping of ABCA4 by mass spectrometry using CID-only fragmentation and HPLC retention time (RT) of glycopepides (GP).

Observed GP mass	RT (min)	Glycan composition	Relative Abundance	Sequence	Glyco site	Theoretical GP mass	Error (ppm)
2688.080	25.41	$Hex_6(HexNAc)_2$	6%	NA**N**STFEELER	N 415	2688.078	0.644
2850.131	25.36	$Hex_7(HexNAc)_2$	52%			2850.130	0.256
3212.185	25.22	$Hex_8(HexNAc)_2$	85%			3012.183	0.574
3174.238	25.17	$Hex_9(HexNAc)_2$	100%			3174.236	0.545
2575.059	32.02	$Hex_6(HexNAc)_3$	10%	DIF**N**ITDR	N 504	2575.055	1.449
2704.102	37.08	$Hex_5(HexNAc)_3(NeuAc)_1$	10%			2704.098	1.379
2866.154	36.86	$Hex_6(HexNAc)_3(NeuAc)_1$	100%			2866.150	1.301
2655.015	37.68	$Hex_6(HexNAc)_3(phos)_1$	14%			2655.021	−2.361
3459.473	36.81	$Hex_3(HexNAc)_3$	100%	CLKEEWLPEFPCG**N**SSPWK	N 1455	3459.476	0.668
3662.559	36.70	$Hex_3(HexNAc)_4$	16%			3662.555	1.122
3409.566	39.36	$Hex_5(HexNAc)_2$	7%	STEILQDLTDR**N**VSDFLVK	N 1527	3409.563	0.968
3571.620	39.30	$Hex_6(HexNAc)_2$	46%			3571.615	1.324
3733.673	39.25	$Hex_7(HexNAc)_2$	70%			3733.667	1.535
3895.725	39.14	$Hex_8(HexNAc)_2$	100%			3895.720	1.214
4057.778	39.09	$Hex_9(HexNAc)_2$	42%			4057.773	1.166
4259.006	51.20	$Hex_4(HexNAc)_2$	3%	LPAPPFTGEALVGFLSDLGQ	N 1586	4258.977	6.880
4421.034	51.08	$Hex_5(HexNAc)_2$	100%	LM**N**VSGGPMTR		4421.030	0.973
4583.113	50.91	$Hex_6(HexNAc)_2$	24%			4583.082	6.705
3637.669	36.27	$Hex_6(HexNAc)_2$	29%	DKNPEEYGITVISQPLNLTK	N 1660	3637.662	1.768
3799.718	36.22	$Hex_7(HexNAc)_2$	11%			3799.714	0.995
3961.772	36.16	$Hex_8(HexNAc)_2$	100%			3961.767	1.093
4123.826	36.05	$Hex_9(HexNAc)_2$	55%			4123.820	1.292

*Glycan compositions on N98 were not available